Published : p. 53 Mat. Res. Soc. Symp. Proc. Vol. 357, 1995

High Resolution Transmission Electron Microscopy of Metallic Film/Laser-Irradiated Alumina Couples

A. J. Pedraza,* Siqi Cao,* L. F. Allard,‡ and D. H. Lowndes

1995

*The University of Tennessee, Knoxville, TN
‡High Temperature Materials Laboratory

Prepared by
Solid State Division
Oak Ridge National Laboratory
P.O. Box 2008
Oak Ridge, Tennessee 37831-6056
managed by
LOCKHEED MARTIN ENERGY SYSTEMS, INC.
for the
U.S. DEPARTMENT OF ENERGY
under contract DE-AC05-84OR21400

HIGH RESOLUTION TRANSMISSION ELECTRON MICROSCOPY OF METALLIC FILM/LASER-IRRADIATED ALUMINA COUPLES.

A. J. PEDRAZA*, SIQI CAO*, L. F. ALLARD** AND D. H. LOWNDES***
*Department of Materials Science and Engineering, The University of Tennessee, Knoxville, TN 37996-2200.
**High Temperature Materials Laboratory, Oak Ridge National Laboratory, Oak Ridge, TN 37831.
***Solid State Division, Oak Ridge National Laboratory, P.O. Box 2008, Oak Ridge, TN 37831-6056.

ABSTRACT

A near-surface thin layer is melted when single crystal alumina (sapphire) is pulsed laser-irradiated in an Ar-4%H_2 atmosphere. γ-alumina grows epitaxially from the (0001) face of α-alumina (sapphire) during the rapid solidification of this layer that occurs once the laser pulse is over. Cross sectional high resolution transmission electron microscopy (HRTEM) reveals that the interface between unmelted sapphire and γ-alumina is atomistically flat with steps of one to a few close-packed oxygen layers; however, pronounced lattice distortions exist in the resolidified γ-alumina. HRTEM also is used to study the metal-ceramic interface of a copper film deposited on a laser-irradiated alumina substrate. The observed changes of the interfacial structure relative to that of unexposed substrates are correlated with the strong enhancement of film-substrate bonding promoted by laser irradiation. HRTEM shows that a thin amorphous film is produced after irradiation of 99.6% polycrystalline alumina. Formation of a diffuse interface and atomic rearrangements that can take place in metastable phases contribute to enhance the bonding strength of copper to laser-irradiated alumina.

INTRODUCTION

The use of metal-ceramic oxides couples is limited by the strength of the interfacial bonding. A thermodynamic model links the bonding strength of the metal-oxide with the heat of formation of the oxide of the metallic component of the couple [1]. The lower the value of the heat of formation the stronger the bond. Under this assumption gold is not expected to react with any oxide because the heat of formation of the gold oxide is positive [2]. However, a very strong bond between gold and silica is developed if the gold is melted on top of fused silica in the presence of oxygen [3].

The body of evidence for metal-oxide bonding presently available strongly suggests that the bonding strength is not only dependent upon thermodynamic parameters, such as the heat of formation, but also upon the chemical and physical conditions of the ceramic surface. Low-energy ion beams have been used to modify the near-surface region of alumina, generating a strong bond to copper [4]. More recently it has been shown that a very strong bond also develops if alumina substrates are pulsed laser irradiated prior to metal deposition. In the case of gold-alumina couples the bonding increases more than 10 times relative to the untreated samples if the laser irradiation is performed under an oxygen atmosphere [5]. For copper-alumina couples the bonding is strongly enhanced if the irradiation is performed at a laser energy density of 1 J/cm^2 in oxygen or in Ar-4%H_2 atmospheres, increasing from 14.5 MPa in the as-received substrates to 73-74 MPa in both cases [6]. At higher laser energy densities the bonding strength of copper-alumina couples rapidly decreases when the substrates are irradiated in an Ar-4%H_2 atmosphere [6].

The electromagnetic radiation of the laser is absorbed at the alumina grain boundaries, impurities and damage sites existing before or generated during the irradiation. Defect sites generated during irradiation are the main source of light absorption In sapphire. The 41 ns pulse produces heating, melting (~0.2 μm) and evaporation in a ~1 μm-thick layer in both alumina and sapphire [7,8,9]. Following irradiation rapid solidification of the melted region takes place.

A strong bond is also produced when metallic films are epitaxially grown on ceramic oxides, e.g. nickel films grown on alumina [10]. The chemical and physical characterization of the metal-oxide interface is vital to understand the bonding process. Several analytical techniques were used

Mat. Res. Soc. Symp. Proc. Vol. 357 © 1995 Materials Research Society

in this research program to study the surface modifications produced in alumina and sapphire by laser irradiation, as well as the corresponding changes in the deposited metallic film. The microstructural and phase changes in the irradiated alumina and in the deposited film, across the interface, were analyzed by cross-sectional transmission electron microscopy (XTEM). The atomic structure of the metal/ceramic interface is being currently analyzed by cross-sectional high resolution transmission electron microscopy (HRTEM). HRTEM images may not provide a unique atomic configuration, due to current limitations in spacial resolution. However, image simulation can help to model the interface and compose the atomic configurations at the interface. Changes in chemical composition that take place at the metal-irradiated oxide interface have been studied using x-ray photoelectron spectroscopy (XPS) [11] and Auger electron spectroscopy (AES) [12]. These changes are another major factor affecting the metal-oxide bonding.

In this paper we report the phase transformations that take place during laser irradiation in alumina and in sapphire. Also initial results are presented on the microstructural changes that take place after copper deposition and annealing of the copper-alumina couples.

EXPERIMENTAL

Commercial alumina substrates of nominal purity 99.6% were irradiated with ten sequential pulses of a XeCl excimer laser (λ=308 nm). All the irradiations were performed at laser energy densities in the range of 1 to 4J/cm^2 in either oxygen or Ar-4%H_2 atmospheres, at a nominal pressure of 1 atm. After irradiation, 80 nm-thick copper films were ion-beam-sputter-deposited from 99.99% pure targets onto the irradiated substrates. The base pressure of the chamber was $1x10^{-6}$ torr and the working pressure was $1x10^{-5}$ torr. After deposition, the metallic film-alumina couples were furnace-annealed at 300 and 500°C for 1 h under a pressure of $1x10^{-5}$ torr.

Cross-sectional TEM samples of metal/ceramic couples were prepared from the laser irradiated regions as follows. i) two pieces of the specimen with interfaces of interest were cemented together, face to face, using a thermal set epoxy, ii) a slab was cut from the cemented sandwich and glued into a brass tube having a 3 mm outside diameter and 2.3 mm inside diameter, iii) thin slices of 3 mm disks were cut from the brass tube with the interface in the middle of the tube (this method eliminates the carbon ring for mounting the cross-sectional sample, and also makes it suitable for low angle ion milling), iv) the specimens were ground to a thickness of 100 μm, v) the ground specimens were dimpled to a thickness of 20 μm or less, vi) the final stage was ion milling of the TEM specimen to perforation.

Ion milling was performed at 6 kV, 1 mA, and 12-14 degrees of milling angle in a liquid nitrogen-cooled stage. The milling rates are quite different for epoxy, metal film, and ceramic substrates. In order to preserve the interface from preferential sputtering during ion milling, the ion beam was partly obstructed, so that the samples were only ion milled from one side of the interface. This permits the ion beam sputtering to proceed from the back of the substrate, while direct exposure of the interface to the ion beam is avoided.

TEM images were recorded on a JEOL 4000EX operated at 400 kV and a Hitachi HF 2000 FEG operated at 200 kV, both equipped with a Gatan slow scan CCD camera for acquiring digitized images.

RESULTS AND DISCUSSION

Laser irradiation of alumina

Figure 1 is an XTEM image of an alumina substrate, laser irradiated at 1J/cm^2 in Ar-4%H_2 atmosphere. A uniform featureless layer of about 0.2 μm-thick was formed after laser irradiation. Convergent beam electron diffraction (CBED) from this layer shows a typical amorphous ring pattern (Fig. 1). The oxygen-to-aluminum concentration ratios detected by energy dispersive x-ray spectroscopy (EDS) from the amorphous region and from the substrate were the same, indicating that the amorphous phase is produced during the rapid solidification of the laser-melted surface alumina layer. A crystalline layer adjacent to the amorphous layer and in contact with the substrate can be seen in fig. 1. This region has a cellular morphology and the same crystallographic orientation as the substrate. This observation indicates that a solidification process had started from the solid substrate but the advancing interface was arrested and the rest of the liquid frozen in

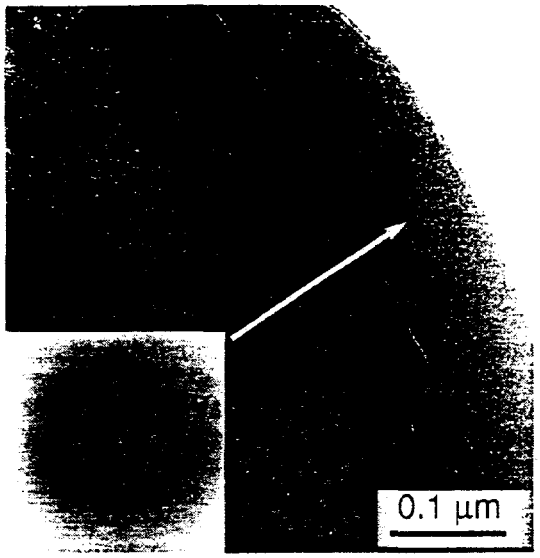

Fig. 1. Amorphous layer formed in alumina after laser irradiation at 1J/cm^2 in Ar-4%H_2. Insert: CBED from amorphous region.

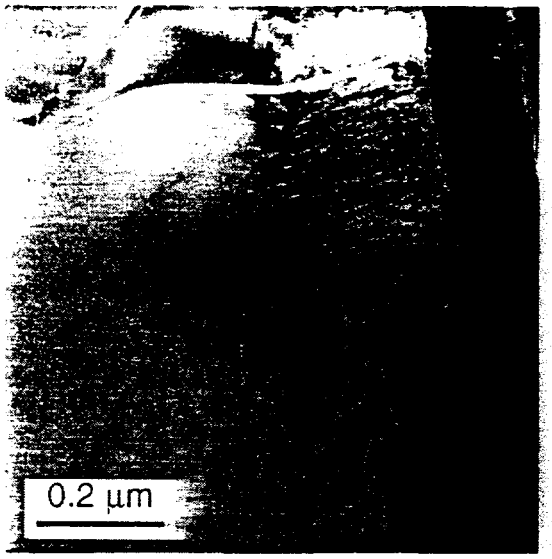

Fig. 2. Melted and resolidified layer in alumina after laser irradiation at 1J/cm^2 in Ar-4%H_2 showing a cellular structure grown from the unmelted substrate.

an amorphous state. The interface arrest cannot be related to a faster cooling of the liquid ahead of the solid-liquid interface because the heat generated during laser processing is dissipated by thermal conduction toward the bulk [8]. A more plausible explanation is that a solute buildup ahead of the advancing interface takes place by solute rejection from the solid. This buildup of solute slows down the solid/liquid interface allowing the rest of the liquid to become amorphous.

The coexistence of a crystallized region with an amorphous layer indicates that minor variations of the deposited energy and local chemical composition can promote a complete layer of either crystalline or amorphous material. In fig. 2, an XTEM of a copper-alumina specimen reveals that in this instance the melted region grew fully crystalline without any amorphous region. This specimen was produced under the same nominal conditions as those shown in figure 1. However, an amorphous layer was observed in a large majority of analyzed specimens irradiated at 1J/cm^2.

On the other hand when the alumina substrates are irradiated at 3J/cm^2 resolidification with columnar grains growing from the substrate proceeds to completion. In some instances small pockets of amorphous material can be seen surrounded by crystalline material (Fig. 3). No extended amorphous region is produced, however, in alumina substrates irradiated at a laser energy density of 3J/cm^2 because the cooling rate in these substrates is slower than in the substrates irradiated at 1J/cm^2.

Another possible reason for the mostly

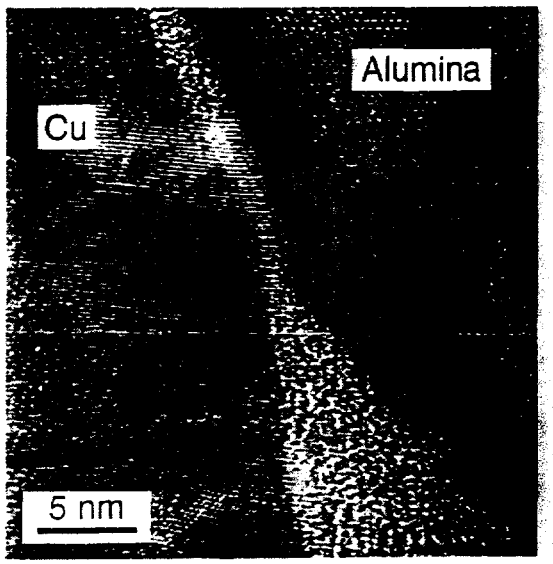

Fig. 3. HRTEM image of an interface between a copper film and an alumina substrate laser irradiated at 3J/cm^2. Notice the amorphous pocket formed from the last-solidified melt.

crystalline phase produced when the substrates are irradiated at a higher laser energy density can be related to the pattern of impurity accumulation in the melted region. Considering that the alumina substrates are melted and resolidified ten times, in each melting cycle the impurities are pushed toward the free surface by the solid/liquid interface. This procedure induces an accumulation of impurities that could ultimately facilitate the amorphization of the surface layer. However, when the irradiation is performed at $3J/cm^2$ significant ablation of the surface layer also occurs [9]. In this way, the removal of a surface layer in each cycle prevents the occurrence of significant impurity accumulation.

Laser irradiation of sapphire

A uniform resolidified layer is produced when c-axis sapphire substrates are laser-irradiated in Ar-4%H_2 at $4J/cm^2$ energy density. Selected area diffraction (SAD) pattern shows that this melted layer is resolidified as γ-alumina, which has a spinel-type cubic structure [13]. The γ-alumina has grown epitaxially from the sapphire substrate with an orientation relationship $(0001)_\alpha//(111)_\gamma$, and $[01\bar{1}0]_\alpha//[1\bar{1}0]_\gamma$. Fig. 4 shows a HRTEM micrograph of a sapphire/γ-alumina interface. The lattice image in the γ-alumina varies significantly due to defects and elastic distortions generated during rapid solidification. The image contrast changes from area to area in the γ-alumina region indicating that there are small misorientations as the melted liquid resolidifies.

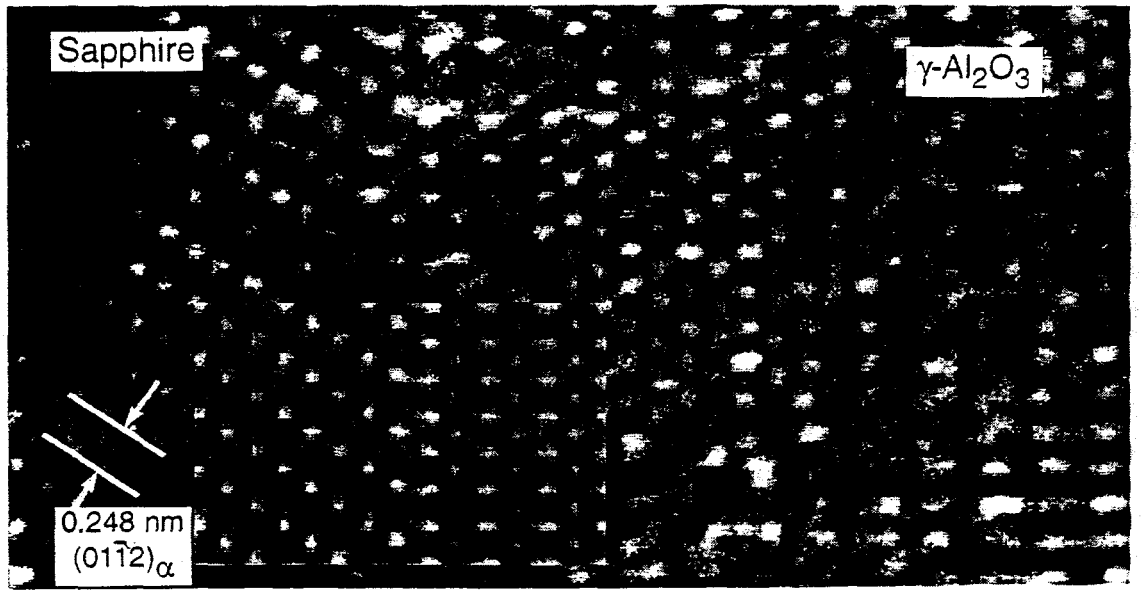

Fig. 4. HRTEM image of sapphire/γ-alumina interface. Insert: simulated interface image (Cs=1.0 mm, defocus=-47 nm, thickness=10 nm).

The interface structure along sapphire/γ-alumina was simulated using the MacTemps image simulation program [14]. The γ-alumina phase is an aluminum deficient spinel structure of the $Fd\bar{3}m$ space group. The oxygen atoms occupy all coordinated (e) sites and aluminum atoms occupy all octahedrally coordinated (d) sites and 2/3 of the tetrahedrally coordinated (a) sites (Wyckoff notation) [15]. At the interface the stacking sequence of close-packed oxygen layers changes from pseudo-hexagonal structure (abab--) of sapphire to cubic structure (abcabc--) of γ-alumina.

The structure of sapphire was simulated first to match the observed HRTEM image in the sapphire region, and then the same parameters were used for interface simulation. The best matched simulation was found by comparing the simulated image to the experimental HRTEM image (see insert in Fig. 4). The atomistic structure of this interface produced by the atom overlay to the simulated image indicates that the interface terminates in an oxygen plane. (Fig. 5).

Copper-ceramic couples

The interface of a copper/alumina couple was investigated after annealing the specimen at 500°C for 1h. In all the cases analyzed in this section the alumina substrates were irradiated at a laser energy density of 1J/cm^2. Selected area diffraction (SAD) of the sputter-deposited copper film produces a ring pattern, indicating that the copper grains have no preferential orientation. Consistently, HRTEM images show no epitaxial relationship between laser irradiated alumina and sputter deposited copper. It is for this reason that lattice images of both copper and alumina at the interface are very difficult to obtain. Also, the need of maintaining edge-on conditions at the interface strongly restricts the stage tilting angles. Fig. 6 shows a HRTEM image of a region that comprises the copper-alumina interface. The alumina substrate is crystalline with a unique orientation, except at the interface where small grains that seem to have originated at that interface grew into the alumina substrate.

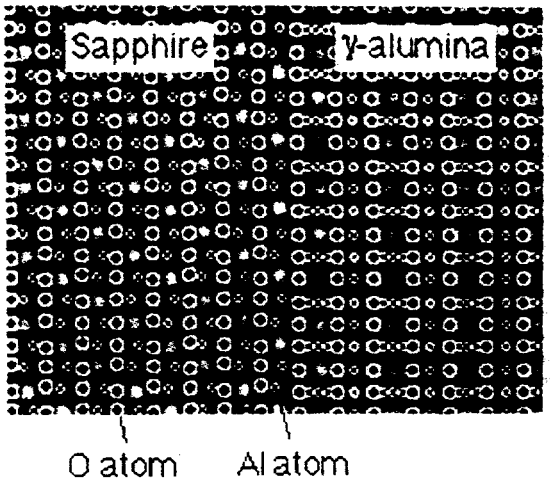

Fig. 5. Simulated HRTEM image of sapphire/ alumina interface with atoms overlay.

There are significant changes in morphology from region to region. Another region of the copper-alumina interface is shown in fig. 7. The original sharp interface has become diffuse. The diffusion of copper in sapphire at 500°C should be negligible [16]. However, we have detected copper in alumina at ~15 nm from the copper-alumina interface. It is possible that copper diffusion into the ceramic is strongly enhanced in the highly defective near-surface region which contains vacancies, dislocations and columnar boundaries.

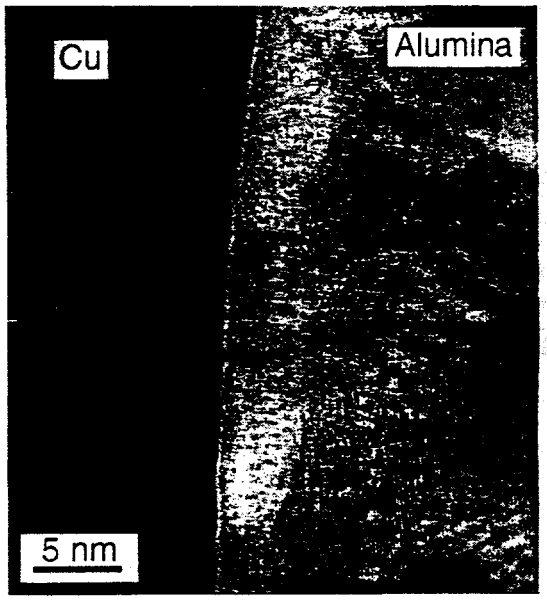

Fig. 6. HRTEM image of an interface between a copper film and an alumina substrate, laser irra diated at 1J/cm^2 after 1h anneal at 500°C. Small crystals can be seen at the interface.

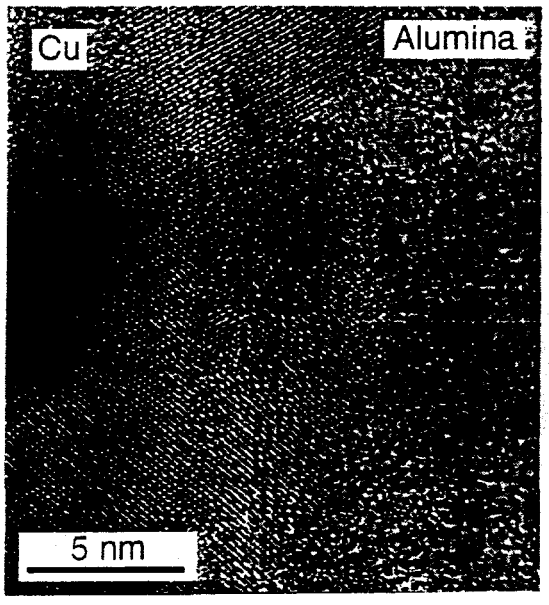

Fig. 7. HRTEM image of an interface between a copper film and an alumina substrate, laser irradiated at 1J/cm^2 after 1h anneal at 500°C, showing a rough interface.

The formation of a diffuse interface should help to increase the bonding strength between the metallic film and the oxide. Also the existence of a disordered region or, more generally, of a region that is far from equilibrium can lead to strong bonding. Thus, atomic relaxations that take place in the amorphous phase during annealing accommodate the metal into lower energy positions further improving the bonding.

CONCLUSIONS

An amorphous layer ~0.2 μm-thick is formed on the near-surface region of alumina after laser irradiation at an energy density of $1J/cm^2$. When the irradiation is performed at an energy density of $3J/cm^2$ the melted region solidifies with the same orientation as the matrix. The crystalline region has a columnar structure, in which the columnar grains are separated from each other by a low angle grain boundary. Also a high dislocation density is observed in the resolidified structure. In some instances resolidified material can be found when the irradiation is performed at $1J/cm^2$ while pockets of amorphous material can be seen in samples irradiated at $3J/cm^2$.

The cubic spinel γ-alumina is formed when sapphire is laser irradiated at $4J/cm^2$.

This study shows that, after annealing, formation of a diffuse interface and atomic rearrangements that can take place in metastable phases contribute to enhance the bonding strength of copper to laser-irradiated alumina.

ACKNOWLEDGMENTS

This research was supported in part by National Science Foundation Grant No. DMR-9116528 and in part by the Division of Materials Science, U.S. Department of Energy and by the U.S. Department of Energy, Assistant Secretary for Energy Efficiency and Renewable Energy, Office of Transportation Technologies, as part of the High Temperature Materials Laboratory User Program, both under contract DE-AC05-84OR21400 with Martin Marietta Energy Systems, Inc.

REFERENCES

1. J. E. MacDonald and J. G. Eberhart, Trans. Met. Soc. AIME, **233**, 512 (1965).
2. W. A. Weyl, in Adhesion and Adhesives-Fundamentals and Practice, edited by J. E. Rutzler and R. L. Savage (John Wiley & Sons, New York, 1953), p. 36.
3. D. C. Moore and H. R. Thornton, J. Res. Natl. Bur. Std., **62**, 127 (1959).
4. J. E. E. Baglin, A. G. Schrott, R. D. Thompson, K. N. Tu, and A. Segmuller, Nucl. Instr. and Method, **B19/20**, 782 (1987).
5. A. J. Pedraza, R. A. Kumar, and D. H. Lowndes, to be published in Appl. Phys. Lett.
6. A. J. Pedraza, M. J. DeSilva, R. A. Kumar, and D. H. Lowndes, to be published.
7. A. J. Pedraza, J.-Y. Zhang, and H. Esron, in Laser Ablation in Materials Processing: Fundamentals and Applications, edited by B. Braren, J. J. Dubowski, and D. P. Norton (Mat. Res. Sco. Proc. **285**, Pittsburgh, PA, 1993) p. 209.
8. A. J. Pedraza and M. J. Godbole, Metallurgical Transactions A, **23A**, 1095 (1992).
9. D. H. Lowndes, M. DeSilva, M. J. Godbole, and D. B. Geohegan, in Laser Ablation in Materials Processing: Fundamentals and Applications, edited by B. Braren, J. J. Dubowski, and D. P. Norton (Mat. Res. Sco.Proc. **285**, Pittsburgh, PA, 1993) p. 191.
10. M. Ruhle, "Misfit Dislocations at Metal/Ceramics Interfaces" presented at the Symposium Cb: Defect-Interface Interactions, MRS Fall Meeting, Boston, MA, Dec. 1993.
11. J. W. Park, A. J. Pedraza, and W. R. Allen, in this proceeding.
12. A. J. Pedraza, J. W. Park, H. M. Meyer III, and D. N. Braski, J. Mater. Res. **9**, 2251 (1994).
13. Siqi Cao, A. J. Pedraza, D. H. Lowndes, and L. F. Allard, Appl. Phys. Lett., **65** (1994) in press.
14. MacTemps Software, Total Resolution, Berkeley, CA 94707.
15. "International Tables for X-Ray Crystallography", **Vol. 1**, edited by N. F. M. Henry and K. Lonsdale (Birmingham, The Kynoch Press, 1969).
16. F. Moya, E. G. Moya, D. Juve, D. Treheux, C Grattepain, and M. Aucouturier, Scripta Metallurgica, **28**, 343 (1993).